

MODELING AND CHARACTERIZATION OF MULTICRYSTALLINE SILICON BLOCKS BY QUASI-STEADY-STATE PHOTOCONDUCTANCE

Mohsen Goodarzi,¹ Daniel Chung,² Bernhard Mitchell,² Thorsten Trupke,² R. A. Sinton,³ and Daniel Macdonald¹

¹Research School of Engineering, The Australian National University, Canberra ACT 2601, Australia

²School of Photovoltaic and Renewable Energy Engineering, UNSW, Sydney, NSW 2052, Australia

³Sinton Instruments Inc., Boulder CO USA. <http://www.sintoninstruments.com>

ABSTRACT: A detailed knowledge of the distributions of carrier lifetimes, impurities and crystal defects in silicon ingots is key for understanding and improving wafer quality, as well as solar cell processing steps. In this work, we have applied a quasi-steady-state photoconductance tester developed for use on ingots for the measurement of lifetimes and dissolved iron concentrations along a p-type multicrystalline silicon block. The iron concentrations are determined by lifetime measurements taken before and after flashing the block to break the iron-boron pairs. The measured iron profile along the block is in qualitative agreement with those reported in previous work, and conforms to the expected trend due to impurity segregation. The impact of non-uniform carrier profiles during the block measurements on the extraction of the Fe profiles are discussed and quantified based on simulations of the quasi-steady-state measurement conditions. The lifetimes are also compared with a calibrated photoluminescence image on the same block, which shows similar qualitative trends, but lower magnitudes due to the lower injection level in the photoluminescence measurement.

Keywords: QSSPC, Carrier Lifetime, Iron concentration, Silicon block.

1. INTRODUCTION

The Quasi-Steady-State Photoconductance (QSSPC) method is well established for measurement of the minority carrier lifetimes on silicon wafers [1]. However, the application of QSSPC methods to ingots, blocks and boules is not as widespread, although it has some attractive advantages in terms of early-stage characterization. For example, knowledge about specific impurities and crystal defects at the ingot level can result in more reliable decisions in regards to the cropping of ingots and blocks for wafering purposes. It would be also possible to sort the wafers at the start of processing and tune the cell process for different quality wafers coming from the different sections of the block [2]. Moreover, accurate details about these characteristics may provide valuable information regarding the manufacturing process to produce higher efficiency or yields in final cells. There have been numerous studies performed on wafers which were cut from different parts of an ingot [3], to provide information about the electronic quality. There have however been fewer studies at the ingot level prior to wafering. Some notable examples include the development of a modified QSSPC tester for applications to ingots and blocks [4], which is also applied in this work, and the recent development of PL-based methods for ingot characterization [5, 6]. This study is focused on the further development of QSSPC methods for applications to ingots, ultimately aiming towards identifying useful correlations between data at the ingot level, such as carrier lifetime and dissolved iron concentrations, and the final cell efficiency.

2. EXPERIMENTAL METHODS AND RESULTS

2.1. Lifetime and Iron Concentration

QSSPC measurements were performed with a BCT-400 measurement system from Sinton Instruments, in QSSPC measurement mode with a 1000-nm IR-Pass Schott glass filter. The sample was an uncropped rectangular block cut from the central part of a standard industrial p-type multicrystalline silicon ingot, with a

square base of 155× 155 mm and a height of 267 mm. There were 20 QSSPC measurement points starting at 10 mm from the bottom edge up to 10 mm from the top edge with a 13 mm gap between each point.

Multiple flashes with a Broncolor Picolite flash with a peak power of 1600 W were used in order to break the FeB pairs in the block. Zoth and Bergholz [7] showed that the interstitial iron concentration in silicon can be calculated from:

$$[Fe] = C \left(\frac{1}{\tau_1} - \frac{1}{\tau_0} \right) \quad Eq. 1$$

Where τ_1 and τ_0 are the measured lifetimes before and after breaking FeB pairs, respectively. The Fe concentration and factor C have been calculated using the method developed in Ref [8].

Lifetime results were also compared with lifetimes measured at UNSW using the PL Intensity Ratio (PLIR) technique [6] which is based on the ratio of two photoluminescence images taken with different spectral filters in front of a CCD camera. This method does not require a separate measurement of the absolute doping density across the height of the brick, and also does not require analysis of the absolute PL signal.

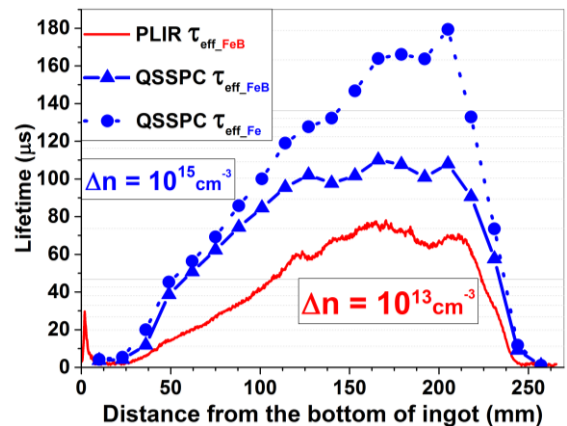


Figure 1: Lifetime vs Block position

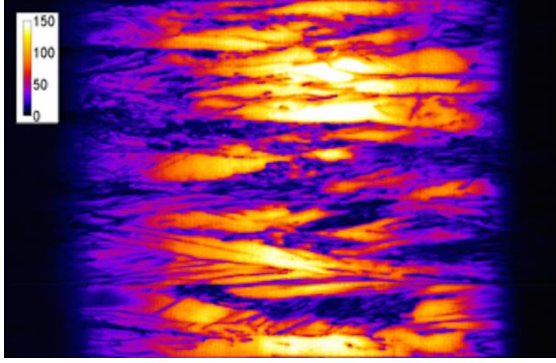


Figure 2: PLIR lifetime image of the block (bottom of brick on the left). The scale bar has units of μs .

Figure 1 shows the QSSPC lifetimes measured along the block both before and after breaking the FeB pairs. The average injection level used here was $\Delta n_{\text{avg}} = 10^{15} \text{ cm}^{-3}$ resulting in an increase in lifetime after breaking the FeB pairs, due to the presence of the lifetime crossover point at around 10^{14} cm^{-3} [9]. The extracted values of τ_{other} are also shown, which represent the lifetime due to all other defects, and these are expected to reflect the lifetime after removal of dissolved Fe due to gettering during cell processing [3]. Also shown are the average carrier lifetimes along the same block as measured by PLIR prior to breaking the FeB pairs. These were measured at a lower injection level, of around $\Delta n_{\text{avg}} = 10^{13} \text{ cm}^{-3}$. Nevertheless, the trend in the PLIR lifetime data is similar to the QSSPC data. The full PLIR lifetime image is shown in Figure 2 illustrating higher lifetimes towards the top of the block.

Figure 3 shows that the interstitial Fe concentration determined from the QSSPC data firstly rapidly decreases along the growth direction from the bottom of the ingot, and then experiences a steady increase in the middle of the ingot. Such a trend has earlier been reported by numerous authors, for example Sinton et al [4] and Mitchell et al [6], and can be explained by solid-state in-diffusion of Fe from the crucible and impurity segregation into the liquid phase during crystallisation, respectively. The boron concentrations determined from the dark conductance measurements are also shown in Figure 3.

To confirm that the difference in the lifetime before and after flashing the block is due to the presence of dissolved Fe, the sample was left in the dark to allow the Fe-B pairs to re-form. QSSPC lifetime measurements were performed during this relaxation period. It has been shown [8] that such lifetime data exponentially decays with an association time constant of τ_{assoc} for wafers containing interstitial Fe. The same approach can be used for ingot measurements, in principle. The results are illustrated in Figure 4 for the collected data from one set of the measurement points on the block.

Tan *et al.* [10] showed the relation between the Fe-B pair formation rate ($\frac{1}{\tau_{\text{assoc}}}$) with the dopant density and the temperature can be expressed as:

$$\tau_{\text{assoc}} = \frac{5.7 \times 10^5}{N_A} T \exp\left(\frac{0.66}{kT}\right) \quad \text{Eq. 2}$$

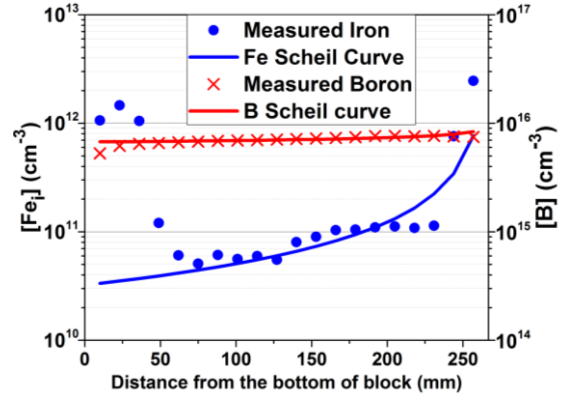


Figure 3: Iron and boron concentration vs block position

Using a dopant density of $7.2 \times 10^{15} \text{ cm}^{-3}$ as measured by the dark conductance and the block temperature (308 K) results in an expected Fe-B pair formation time of approximately 26 mins. This compares well with the measured re-pairing time of 28 mins extracted from fitting the lifetime data in Figure 4 (note that the data is for a single point where lifetime was higher than the block average). This confirms that the observed changes in lifetime are indeed due to the presence of interstitial Fe.

2.2. Comparison to Scheil Equation

To confirm the extracted Fe and B profiles in our study, the results were compared with Scheil's segregation model for impurities and dopants during ingot growth. The boron profile along the block was extracted from the resistivity profile. Figure 3 presents the expected concentration of boron, with a segregation coefficient of 0.8, and iron, with a segregation coefficient of 6.2×10^{-3} [11], along the ingot as a function of the ingot height respectively. Since the Fe concentration depends on mechanisms other than segregation at the two ends of the ingots, the extracted values below 25% of the total height and above 80% of the total height of the ingot were not used in fitting the Scheil model. The boron and Fe profiles are in reasonable agreement with those expected from the Scheil equation, and with those reported in other studies [12].

3. MODELING OF QSSPC MEASUREMENTS

Cuevas [13] proposed a model to simulate Quasi-Steady State (QSS) photoconductance measurements in silicon wafers, utilizing numerical analysis in order to determine Δn profiles for typical wafer thicknesses. Here we use a similar approach to model QSSPC measurements in much thicker samples such as slabs, bricks and blocks. It should be noted that the key difference is the sample thickness, whereby minority carrier currents do not reach the rear surface, and so the carrier profiles are always highly non-uniform.

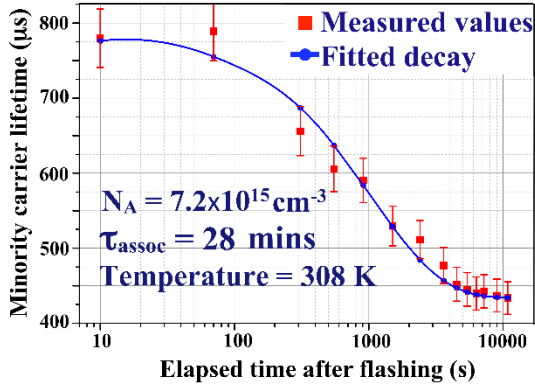


Figure 4: Reduction in lifetime during the re-pairing of FeB pairs

A first step is to simulate the generation profile within the sample depth for different light sources. Carrier recombination and diffusion are then simulated to allow the steady-state excess carrier density Δn profile to be determined. From these profiles, the average lifetime and excess carrier density extraction is performed in the same way as implemented in the QSSPC tool, producing a full simulation of the measurement process.

An example of the modeled generation profile and two excess carrier profiles are shown in Figure 5. Clearly the Δn profile in an ingot is non-uniform, and so an average value is required for the data analysis. Bowden and Sinton [2] introduced methods to estimate Δn_{avg} and W_{eff} (the effective thickness) which are utilized in both the QSSPC tool, and in the simulations used here.

The model is explained in detail in an upcoming publication, where it is shown how the Δn profile can be used to determine the value for Δn_{avg} and to ultimately calculate the effective bulk lifetime (τ_{eff}) at different average injection levels (Δn_{avg}), where τ_{eff} is:

$$\frac{1}{\tau_{eff}} = \frac{1}{\tau_{SRH_{Fe}}} + \frac{1}{\tau_{SRH_{FeB}}} + \frac{1}{\tau_{Auger}} + \frac{1}{\tau_{Other}} \quad Eq. 3$$

Interstitial Fe and FeB pair recombination parameters can be used in the model to calculate the relevant injection dependent Shockley Read Hall lifetimes. These values can be changed to simulate lifetime measurements taken on ingots before and after breaking the Fe-B pairs, in order to estimate the interstitial iron concentration. Figure 5 shows excess carrier density profiles for a sample with $[Fe] = 5 \times 10^{11} \text{ cm}^{-3}$ illuminated under 10 suns. The lifetime crossover point is evident at the expected value of 10^{14} cm^{-3} .

The accuracy of the Bowden and Sinton approximations are validated in our upcoming work in detail. The simulation tool allows us to demonstrate that the errors resulting from the non-uniform carrier profiles in the calculation of the interstitial iron concentration are relatively small ($< 40\%$) in most practical cases. It is also shown the value of τ_{other} , Δn_{avg} and $[Fe]$ can affect the accuracy in different ways. However, $[Fe]$ itself is the most significant source of error, which can introduce up to 40% error in the typical Fe concentration range.

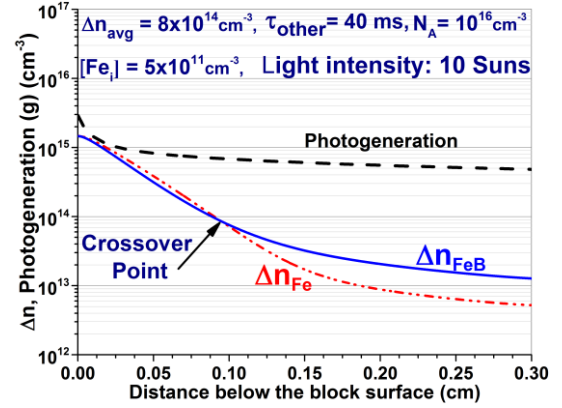


Figure 5: Excess carrier density and photogeneration vs distance below surface of block

4. CONCLUSIONS

This paper presents our preliminary results on applying the QSSPC method for silicon ingot characterization for solar cells. Comparison with PL lifetime imaging on the same ingot reveals notably higher lifetime values measured with QSSPC, due to the large difference in the injection levels at which each measurement was performed.

The main findings in terms of lifetime and dissolved Fe concentrations along the ingot are qualitatively similar to those previously reported [4]. The measured FeB re-pairing time is consistent with that expected from the dopant concentration, and confirms the presence of dissolved Fe and its effect on the minority carrier lifetime in the ingot. Extracted iron and boron concentrations were in reasonable agreement with the Scheil equation for segregation.

We have developed a simulation tool which models the generation and excess carrier profiles depth-wise, in order to calculate the effective lifetime determined by the QSSPC tool along the block. The results, which will be published in detail elsewhere, indicate that the non-uniform carrier profiles only introduce small errors in the resulting Fe concentrations (usually less than 40%), and that these can be corrected for in any case.

Future work will attempt to study the usefulness of the lifetime and dissolved Fe analyses at the ingot level for various types of ingots, with the final aim to establish correlations between the ingot level data and final cell performance.

ACKNOWLEDGEMENTS

This project has been supported by the Australian Renewable Energy Agency (ARENA) through project RND009.

5. REFERENCES

- [1] R. A. Sinton and A. Cuevas, "Contactless determination of current-voltage characteristics and minority-carrier lifetimes in semiconductors from quasi-steady-state photoconductance data," *Applied Physics Letters*, vol. 69, p. 2510, 1996.
- [2] S. Bowden and R. A. Sinton, "Determining lifetime in silicon blocks and wafers with accurate expressions for

- carrier density," *Journal of Applied Physics*, vol. 102, p. 124501, 2007.
- [3] L. Geerligs, "Impact of defect distribution and impurities on multicrystalline silicon cell efficiency," in *Photovoltaic Energy Conversion, 2003. Proceedings of 3rd World Conference on*, 2003, pp. 1044-1047.
- [4] R. Sinton, T. Mankad, S. Bowden, and N. Enjalbert, "Evaluating silicon blocks and ingots with quasi-steady-state lifetime measurements," in *Proceedings of the 19th European Photovoltaic Solar Energy Conference, Paris, France*, 2004, pp. 520-523.
- [5] B. Mitchell, T. Trupke, J. W. Weber, and J. Nyhus, "Bulk minority carrier lifetimes and doping of silicon bricks from photoluminescence intensity ratios," *Journal of Applied Physics*, vol. 109, p. 083111, 2011.
- [6] B. Mitchell, D. Macdonald, J. Schon, J. W. Weber, H. Wagner, and T. Trupke, "Imaging As-Grown Interstitial Iron Concentration on Boron-Doped Silicon Bricks via Spectral Photoluminescence," *IEEE Journal of Photovoltaics*, vol. 4, pp. 1185-1196, 2014.
- [7] G. Zoth and W. Bergholz, "A fast, preparation-free method to detect iron in silicon," *Journal of Applied Physics*, vol. 67, pp. 6764-6771, 1990.
- [8] D. Macdonald, L. Geerligs, and A. Azzizi, "Iron detection in crystalline silicon by carrier lifetime measurements for arbitrary injection and doping," *Journal of Applied Physics*, vol. 95, pp. 1021-1028, 2004.
- [9] D. Macdonald, T. Roth, P. N. K. Deenapanray, T. Trupke, and R. A. Bardos, "Doping dependence of the carrier lifetime crossover point upon dissociation of iron-boron pairs in crystalline silicon," *Applied Physics Letters*, vol. 89, p. 142107, 2006.
- [10] J. Tan, D. Macdonald, F. Rougieux, and A. Cuevas, "Accurate measurement of the formation rate of iron-boron pairs in silicon," *Semiconductor Science and Technology*, vol. 26, p. 055019, 2011.
- [11] G. Coletti, D. Macdonald, and D. Yang, "Role of Impurities in Solar Silicon," in *Advanced Silicon Materials for Photovoltaic Applications*, ed: John Wiley & Sons, Ltd, 2012, pp. 79-125.
- [12] D. Macdonald, A. Cuevas, A. Kinomura, Y. Nakano, and L. J. Geerligs, "Transition-metal profiles in a multicrystalline silicon ingot," *Journal of Applied Physics*, vol. 97, p. 033523, 2005.
- [13] A. Cuevas, "Modelling silicon characterisation," *Energy Procedia*, vol. 8, pp. 94-99, 2011.